



ELSEVIER

Journal of Electron Spectroscopy and Related Phenomena 95 (1998) 255–260

JOURNAL OF
ELECTRON SPECTROSCOPY
and Related Phenomena

Input electron optics for Mott detectors used in secondary electron magnetometry

L. Duò*, M. Marcon, F. Ciccacci

INFM — Dipartimento di Fisica, Politecnico di Milano, piazza L. da Vinci 32, 20133 Milan, Italy

Received 8 May 1998; accepted 8 July 1998

Abstract

An electron spin polarization detector to be used in thin film and surface magnetometry via secondary electron emission is described in detail. It consists of a Mott detector coupled to an input electron optic designed to improve the overall efficiency of the system. This is achieved by taking full advantage of the polarization increase for electrons emitted at low kinetic energy, generally observed in ferromagnets. The input electron optic is appositely designed so as to operate as an energy low pass filter, which strongly modifies the energy distribution of the secondary electrons collected by the Mott detector. Ray tracing analysis indicates that the system performances are improved by more than a factor of 3 with respect to a bare detector operating with an undistorted secondary electron spectrum. © 1998 Elsevier Science B.V. All rights reserved.

Keywords: Electron optics; Secondary electron emission; magnetometers

1. Introduction

When a solid is irradiated with a beam of monochromatic primary electrons of moderate kinetic energy E_p (up to a few keV), aside from particular excitations (e.g. core excitations at thresholds, Auger decays, energy losses), the spectrum of the emitted electrons is characterized at low energies by a large and broad peak of secondary electrons, and at the high energy side by the elastically reflected electrons. In the intermediate region, a mixture of cascade electrons and rediffused primaries is emitted.

In the case of a ferromagnetic solid, the cross-sections for inelastic scattering due to electron–hole pair creation exhibit large spin dependencies due to exchange scattering. These lead to scattering asymmetries, which signal the presence of long-range

magnetic order and whose magnitude is related to the average band magnetization of the sample [1, 2]. These characteristics make spin polarized secondary electron spectroscopy (SPSES) an interesting tool for magnetometry with the further peculiarity of surface sensitivity, intrinsic to the electronic probe. The relevant quantity detected by SPSES, i.e. the spin polarization P , is defined as $P = (n \uparrow - n \downarrow) / (n \uparrow + n \downarrow)$, where $n \uparrow$ ($n \downarrow$) is the number of emitted electrons with magnetic moment parallel (antiparallel) to the sample magnetization.

Opposite to a naive picture, according to which the spin polarization P at low energy would equal the average valence band polarization, P was found to depend on the secondary kinetic energy E with a similar decreasing behavior for all 3d ferromagnets [1]. At low kinetic energy, due to the relevance of the exchange scattering in the close vicinity of the Fermi level (E_F), P shows a strong monotonic

* Corresponding author; e-mail: lamberto.duo@fisi.polimi.it.

decrease (up to a factor of three in Ni(110) on going from 0 to 10 eV [3]) for increasing E , reaching a plateau above ~ 10 eV. This polarization plateau is known to correspond to the total polarization of the valence band and thus can be identified as the sample magnetization averaged in space over the range of secondary electron emission. The low energy enhancement displayed by P is attributed to preferential inelastic scattering of spin-down electrons leading to a higher escape probability for spin-up electrons [4]. At higher energy, P keeps slowly decreasing because an increasing fraction of re-emerging unpolarized primary electrons is able to undergo multiple losses.

The behavior of P versus E is generally measured by exciting the sample with a standard monochromatic electron gun. The emitted electrons are then selected with an energy analyzer to which a polarimeter (typically a Mott detector) is coupled for the detection of the electron spin [5]. For magnetometry purposes, the details of P versus E are not relevant and information integrated over energy is needed. This makes the system much simpler, i.e. without the need of the electron analyzer, giving a much broader solid angle for the collection of the emitted electrons. From this point of view, the energy dependence of P , even if it prevents an absolute measurement of the magnetization because of the unknown converting factor between P and the average valence band polarization, can be exploited to maximize the sensitivity of the magnetometer. As in many spin-resolved spectroscopies, the relevant figure of merit (FOM) is proportional both to the squared effective polarization, i.e. to the average polarization over the energy range detected by the apparatus, and to the secondary electron yield, which is the ratio between the number of emitted secondary electrons and the number of incoming electrons [6]. As a matter of fact, with an experimental set-up which does not use the electron analyzer, a very small primary electron current ($< 1 \mu\text{A}$) is sufficient to saturate the detectors of the polarimeter. As a consequence, it turns out that the best performances in terms of sensitivity are obtained, for a given magnetization, by collecting only the electrons emitted at very low energy (< 10 eV).

In this work, we present an apparatus for magnetometry based on a low energy (10–25 keV) Mott polarimeter equipped with two electron counters.

The transport electron optic is designed in such a way to maximize the magnetometer FOM by acting as a simple and efficient low pass filter. While at very low energy (up to a fraction of an eV) all the emitted electrons are able to reach the target of the Mott polarimeter, the transmission at 10 eV is about two orders of magnitude smaller. The monotonic decrease of the optic transmission versus E is such that at the typical energy of the elastic peak, the emitted intensity is suppressed by a further decade.

2. Polarization detector

2.1. Layout

The schematic view of the polarization detector is shown in Fig. 1. It is made of a spin analyzer based on Mott scattering and a transport electron optic in front of it. The miniature Mott polarimeter, mounted on a CF 150-(ID) flange, has been designed and realized at the University of Edinburgh. Its description can be found in Refs. [7, 8]. For the sake of completeness, we just give here the relevant characteristics of it. The central components of the analyzer are two electrically isolated concentric hemispheres, the outer one of internal radius 50 mm and the inner one of external radius 25 mm. The first hemisphere is operated at 1200 V, while the second works at 10–25 kV. A gold foil 2 mm thick is mounted at the center of the inner hemisphere and electrically connected to it. The electron beam enters the polarimeter through a 5 mm aperture in the outer hemisphere and is then focused by the strong radial field through a 3 mm aperture in the inner hemisphere onto the center of the Au target. Electrons scattered through $\pm 120^\circ$ from the foil exit the inner hemisphere via two 10 mm apertures (not shown in Fig. 1). They are then decelerated by the radial field and exit the outer hemisphere towards two microchannel-plate electron counters (not shown in Fig. 1). The retarding field filters out electrons which have lost more than $\Delta E = 1300$ eV, so that only electrons scattered quasi-elastically are detected. The chosen value of ΔE for the maximum energy loss represents a good compromise between the need for a high counting rate, which increases with increasing ΔE , and for a high asymmetry

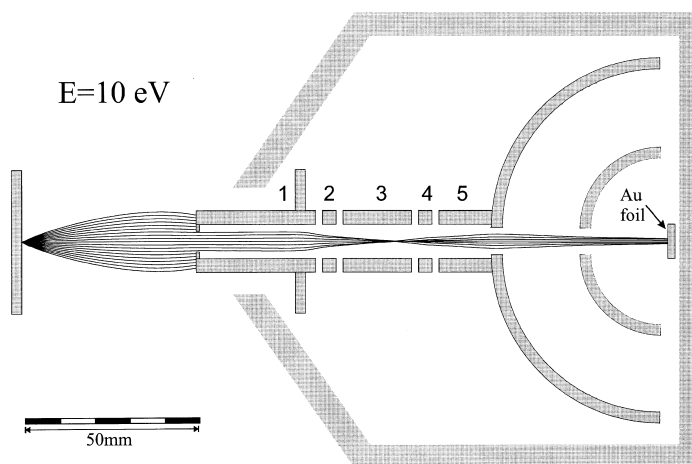


Fig. 1. Schematic view of the Mott detector with the transfer electron optics. The calculated trajectories are shown for a point source emitting electrons at $E = 10$ eV within $\pm 30^\circ$ from the normal at steps of 5° . The potentials are 260 V, 1500 V, 1100 V, 300 V, and 1200 V for electrodes 1–5, respectively. The outer hemisphere is at the same potential as electrode 5 (1200 V). The inner hemisphere is at the same potential as the Au target (15 kV). The case and the sample are grounded.

between the scattering at $+120^\circ$ and -120° , which instead decreases with increasing ΔE [8, 9].

In front of the Mott detector and attached to it, an input electron optic consisting of five electrodes is placed, as shown in Fig. 1. The electrodes are cylindrical elements made of aluminum whose inner diameter is 10 mm, apart from the first element, closer to the sample, which has a smaller front aperture (7 mm). The reduced aperture of the first electrode has the aim of preventing the electron beam entering the optic and hitting the inner surface of the electrodes during its trajectory to the target. This is particularly important because the impact of an electron against the inner wall of the optic can result in a large amount of secondary electrons which may be able to reach the detectors, causing, therefore, a strong artifact. The electrical and mechanical separation of the electrodes is achieved by means of 2 mm sapphire balls located in appropriate holes on each side of the electrodes. Care has been taken to avoid a direct view of the insulating parts from the electron beam. The entire assembly is held together by three screws, resulting in a compact and mechanically stable structure. The electrode bias voltages are obtained by means of a single power supply fed into a multi-output divider box containing high precision potentiometers. The whole detector is then surrounded by a grounded stainless steel shield in order to prevent the presence

of stray fields outside it and to avoid direct view of the electron beam toward the outer surface of the electrodes. This has to be taken into account since, due to the low bias current imposed by the d.c. supply, a small current variation across the electrodes can cause significant voltage variations with respect to those given when no electrons hit the electrodes.

The input electron optic has been designed in such a way to satisfy the following requirements: (i) a focus on the gold target of the Mott detector, for a correct operation; (ii) an energy low pass filtering effect as discussed in the next section. We have used electron trajectory simulation based on the ray-tracing program SIMION [10] to optimize electrode voltages. Their value, with respect to ground (i.e. to the shield and the sample) are 260 V, 1500 V, 1100 V, 300 V, and 1200 V for electrodes 1–5, respectively. In this way, the last electrode is at the same potential as the outer hemisphere. Furthermore, the third electrode has been supplied with four deflection plates (with ± 50 V for the x and y deflections) in order to correct for possible misalignments. In Fig. 1, electron trajectories emitted from a point source having an angular divergence of $\pm 30^\circ$ and a typical energy of 10 eV are shown. They indicate the presence of two focusing planes: the first one in the middle of the third electrode and the second one at the Au target, as requested. For a circular source of 6 mm diameter and 10 eV energy,

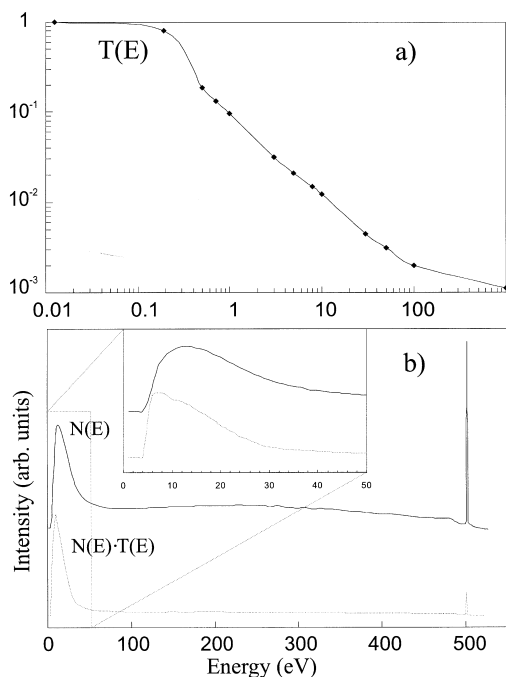


Fig. 2. (a) Calculated transmission function $T(E)$ versus E of the transfer optics for an isotropic point source placed 50 mm from the first electrode entrance. (b) (—) energy distribution curve, $N(E)$, measured for Fe with a primary energy $E_p = 500$ eV; (⋯) energy distribution curve after the electron optics filtering, $N(E)T(E)$. Inset: secondary region for the $N(E)$ and the $N(E)T(E)$ profiles. In both cases, the spectra have been normalized to the same peak intensity and shifted on the vertical coordinate.

the electrons entering the optic hit the Au target with a spot size of less than 2 mm diameter and an angular divergence of less than $\pm 2.5^\circ$. These figures are weakly dependent on the electron energy and on the Au target voltage. Fig. 1 clearly shows that some of the electrons hit the external surface of the first optic element. To avoid the current limit problems discussed above, a decoupling buffer is placed in the resistive chain in correspondence with the first electrode output voltage.

2.2. Energy filtering

The attractive effect on the emitted electrons caused by the positive voltage of the first electrode is clearly revealed in Fig. 1. The interesting aspect is, however, represented by its strong dependence upon energy in terms of collection angle. Before showing the results

of a full SIMION analysis for this problem, it may be worth briefly discussing, in an algebraic way, the energy filtering effect by using the simple approximation of a uniform field between the sample and the first electrode. In the low kinetic energy (E) limit, we can consider parabolic trajectories between the sample and the first electrode. Calling L ($= 50$ mm) the distance between the source and the first electrode and d ($= 7$ mm) the diameter of the first aperture, the transmission (T) is simply calculated to be $T = 1$ for

$$E < \frac{e\Delta V}{16} \left(\frac{d}{L}\right)^2 = 0.32 \text{ eV}$$

where e is the electron charge and $\Delta V = 260$ V is the potential difference between the first electrode and the sample. On the other hand, in the high energy limit $E \gg e\Delta V$, where basically linear trajectories occur, it turns out that

$$T = \frac{1}{8} \left(\frac{d}{L}\right)^2 = 2.5 \times 10^{-3}$$

In Fig. 2(a), the transmission of the electron optic is displayed versus E for an isotropic point source as obtained by the SIMION simulation. In agreement with the approximate analysis given above, it can be seen that while electrons with energy up to ~ 0.2 eV are collected within an emission angle of $\pm 90^\circ$, a strong reduction of the optic transmission is evidenced at higher energy. A sensitivity analysis has shown that the optic transmission is not appreciably modified up to a spot diameter of 10 mm and a ± 10 mm variation of the sample working distance. As a consequence, misalignments between the sample spot and the optic axis are also not particularly dangerous.

To test the improvement of the magnetometer FOM due to the energy filtering effect, with respect to a constant optic transmission, an analysis based on the energy distribution curve $N(E)$, i.e. the number of electrons emitted for a given primary energy normalized to the total emitted current, and on polarization $P(E)$ has been made. The idea is that the FOM is proportional to the squared product of $N(E)T(E)P(E)$ integrated over energy in the $0-E_p$ range, normalized to the total current reaching the Au target, which is the integral of $N(E)T(E)$ over the same range.

For the simulation, $N(E)$ has been taken by measuring the energy loss spectrum from a Fe sample. A primary energy $E_p = 500$ eV has been chosen considering that this value maximizes the true secondary electron yield [5], which is the number of emitted secondary electrons (with kinetic energy below ~ 50 eV) divided by the number of incoming primary electrons. The spectrum has been recorded by means of a cylindrical mirror analyzer with a fixed pass energy, in order to keep the same instrumental resolution during the scan. In this way, the analyzer transmission decreases with energy in a $1/E$ fashion [11]. In Fig. 2(b) (solid line), the true $N(E)$ function is displayed after correcting the raw data to restore a constant analyzer transmission. This spectrum is characterized by a large and broad secondary intensity centered at ~ 12 eV and a sharp peak of elastic electrons at E_p . To qualitatively show the strong filtering effect, in Fig. 2(b) (dotted line), the $N(E)T(E)$ function is shown as well, normalized to the same peak intensity as $N(E)$. In this case, the elastic peak is nearly vanished and the secondary peak is much narrower and centered at lower energy (~ 8 eV) if compared to the $N(E)$ profile, as shown in the inset of Fig. 2(b).

Concerning the polarization dependence upon E , we have used published data on an iron rich magnetic glass, namely $\text{Fe}_{83}\text{B}_{17}$ [5], which are the only $P(E)$ results reported on the whole 0 – E_p energy range, to our knowledge. The above analysis shows that the FOM improves by a factor of ~ 3 due to the effect of the filtering optic with respect to a constant transmission of the input optic. It has to be noted that the polarization of $\text{Fe}_{83}\text{B}_{17}$ shows a weak energy dependence in the 0 – 10 eV range with a reduction less than a factor of two for $P(E)$ [5], as compared, for example, with a three times reduction for Ni, as mentioned. Therefore, the three times larger sensitivity towards magnetization found for this polarization detector has to be regarded as a lower limit.

Finally, we note that if the primary energy E_p is large enough (typically $E_p > 500$ eV [5]), the penetration depth is larger than the typical escape depth for secondary electrons. This means that in SPSES, the probing depth of the experiment is determined by the escape depth and is independent of E_p . In the present case, the filtering optic is made in such a way as to give an average kinetic energy lower than 10 eV (see inset in Fig. 2(b)). According to the present

knowledge on electron inelastic mean free path inside a solid [4, 12], these electrons have a typical escape depth of ~ 20 Å. In this situation, considering that in the important issue of magnetism in thin films and multilayers the relevant thickness can be down to a few atomic layers (i.e. a few Å), it would be rather important to decrease the probing depth of the magnetometer. This may be achieved with our polarimeter just by imposing a positive bias to the sample. This prevents the lower energy electrons to enter the optic. For a given sample bias V_s , the optic transmission goes to zero up to an energy threshold value and suddenly reaches a maximum. At higher energy T is similar to that for the grounded sample (Fig. 2(a)). The energy at which the transmission maximum occurs increases for increasing V_s . As an example, for $V_s = 100$ eV, the average kinetic energy of the electrons entering the optic is ~ 30 eV, giving a very small escape depth of ~ 5 Å. This means that by varying V_s , the surface sensitivity of the magnetometer can be easily tuned. In case of a thin magnetic film deposited on top of a non-magnetic substrate, this also improves the FOM since the decrease of the average P is largely overcompensated by the increased sensitivity towards the electrons coming from the topmost layer.

Acknowledgements

We thank U. Del Pennino for making available the energy loss data.

References

- [1] H.C. Siegmann, E. Kay, in: J.A.C. Bland, B. Heinrich (Eds.), *Ultrathin Magnetic Structures*, Vol. 1, Springer-Verlag, Berlin, 1994, p. 152.
- [2] M. Landolt, R. Feder (Eds.), *Polarized Electrons in Surface Physics*, World Scientific, Singapore, 1985, p. 385.
- [3] H. Hopster, R. Raue, E. Kisker, G. Güntherodt, M. Campagna, *Phys. Rev. Lett.* 50 (1983) 71.
- [4] H.C. Siegmann, *J. Phys. C* 4 (1992) 8395; G. Schönense, H.C. Siegmann, *Ann. Phys.* 2 (1993) 465.
- [5] D. Mauri, R. Allenspach, M. Landolt, *J. Appl. Phys.* 58 (1985) 906.
- [6] J. Kessler, *Polarized Electrons*, 2nd edn., Springer-Verlag, Berlin, 1985.

- [7] F. Ciccacci, S. De Rossi, D.M. Campbell, *Rev. Sci. Instrum.* 66 (1995) 4161.
- [8] S. Watkin, D.M. Campbell, P.S. Farago, unpublished work.
- [9] T.J. Gray, F.B. Dunning, *Rev. Sci. Instrum.* 63 (1992) 1635.
- [10] SIMION 3D, version 6.0, Idaho National Engineering Laboratory, P.O. Box 1625, Idaho Falls, ID 83415, 1995.
- [11] P.W. Palmberg, *J. Vac. Sci. Technol.* 12 (1975) 379.
- [12] M.P. Seah, W.A. Dench, *Surf. Interf. Anal.* 1 (1979) 2.